Local Coulomb Explosion of Boron Nitride Nanotubes under Electron Beam Irradiation

Xianlong Wei,[†,*] Dai-Ming Tang,[‡] Qing Chen,[†] Yoshio Bando,[‡] and Dmitri Golberg[‡,*]

[†]Key Laboratory for the Physics and Chemistry of Nanodevices and Department of Electronics, Peking University, Beijing 100871, People's Republic of China, and [‡]International Center for Materials Nanoarchitectonics (MANA), National Institute for Materials Science (NIMS), Namiki 1-1, Tsukuba, Ibaraki 305-0044, Japan

ABSTRACT

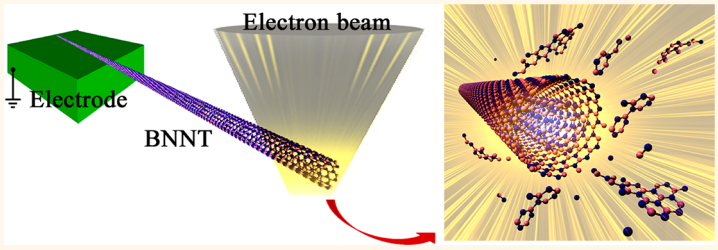

In many previous reports, the engineering of nanostructures using electron beam irradiation (EBI) in a high vacuum has primarily been based on the knock-on atom displacement. Herein, we report a new phenomenon under EBI that can also be effectively used to engineer a nanostructure: local Coulomb explosion (LCE) of cantilevered multiwalled boron nitride nanotubes (BNNTs) resulted from their profound positive charging. The nanotubes are gradually shortened, while the tubular shells at free ends are torn into graphene-like pieces and then removed during LCE. The phenomenon is dependent not only on the characteristics of an incident electron beam, as in the case of a common knock-on process, but also on the cantilevered tube length. Only after the electron beam density and tube length exceed the threshold values can LCE take place, and the threshold value for one of the parameters decreases with increasing the value of the other one. A model based on the diffusion of electron-irradiation-induced holes along a BNNT is proposed to describe the positive charge accumulation and can well explain the observed LCE. LCE opens up an efficient and versatile way to engineer BNNTs and other dielectric nanostructures with a shorter time and a lower beam density than those required for the knock-on effect-based engineering.

KEYWORDS: local Coulomb explosion · boron nitride nanotube · structure engineering · electron beam irradiation

Boron nitride nanotubes (BNNTs), a structural equivalent of carbon nanotubes (CNTs) with alternating B and N atoms substituting for C atoms in a honeycomb lattice, exhibit comparable mechanical performance but completely different electrical properties as compared to CNTs.[1,2] While CNTs are metallic or semiconducting depending on their chirality, BNNTs are insulators with a band gap of about 5.5 eV, independent of their atomic structures.[1] With 1D tubular character and outstanding elastic and tensile properties, BNNTs, similar to CNTs, are thought to be promising for a variety of applications, such as nanoprobes for sensing, imaging, and nanomanipulation, key components for building nanomechanical systems and reinforcements in composites, especially in the cases requiring insulating and structure-insensitive materials. For all of those applications, it is highly important to use BNNTs with a specific length. However, to date, in contrast with many well-developed methods for engineering CNT lengths,[3,4] an efficient method for engineering the length of BNNTs is still not available.

Electron beam irradiation (EBI) is as a powerful tool for engineering the nanostructures and modifying their physical properties. The engineering of nanostructures with EBI and the effects of EBI on nanostructures have intensively been studied in recent years.[5,6] One of the primary effects of EBI is the knock-on displacements of targeting atoms due to the elastic collisions with high-energy incident electrons.[7] This can locally modify the structures of irradiated

* Address correspondence to weixl@pku.edu.cn, golberg.dmitri@nims.go.jp.

Received for review January 26, 2013 and accepted March 4, 2013.

Published online March 04, 2013
10.1021/nn400423y

targets down to the atomic level, and the previously reported engineering of nanostructures using EBI has mostly been based on this effect, especially for the *in situ* engineering inside a transmission electron microscope (TEM) under an ultrahigh vacuum.[3,5,6] The knock-on atom displacement in BNNTs and the related effects have also been studied. Zobelli *et al.* found that divacancies had primarily been formed in BNNTs under electron irradiation, and these tended to be clustered into extended defects locally changing the nanotube diameter and chirality but not the physical properties.[8] These authors also used electron irradiation to reshape single-walled BNNTs.[9] Stéphan *et al.* found that BNNT shells could be transformed to small BN cages under EBI.[10] Recently, postsynthesis C doping of BNNTs for engineering tube electrical properties using EBI was also achieved by us.[11,12] By adopting intense EBI, the knock-on atom displacements can result in severe local atom sputtering from the irradiated area; this has been used to cut various nanostructures and to engineer their length. Cutting of BNNTs and their length modulations based on the knock-on effect have been achieved by Celik-Aktas *et al.*[13] However, it is a relatively tough task. The cutting of a multiwalled BNNT about 12−80 nm thick took the irradiation time as long as 0.5−2 h under a huge beam density of 300 A/cm^2.[13]

Herein, we report a new interesting phenomenon primarily caused by profound BNNT positive charging under EBI, namely, a local Coulomb explosion (LCE) of cantilevered BNNTs, where BNNTs were gradually shortened with the tubular shells at their free ends being torn into pieces and then removed. Since tube shortening by LCE takes a much shorter time and can occur at a much lower beam density than those required for the knock-on effect-based cutting, it provides a more efficient method for engineering the BNNT lengths. In addition to a normal dependence on the characteristics of incident electron beam, similar to a knock-on process, LCE also depends on the length of a cantilevered BNNT in our particular experimental setup. Only after electron beam density and tube length are larger than some threshold values can LCE take place.

RESULTS AND DISCUSSION

As schematically shown in Figure 1a, the tubular shells at the free end of a cantilevered BNNT protruding from a Au electrode were observed to be torn into small pieces and then removed when the tube was irradiated by the electron beam with a high enough intensity. Figure 1b−e shows the TEM images of a cantilevered BNNT under EBI when the electron beam density was gradually increased by decreasing a beam size at a fixed magnification. At the beginning, the beam size was so large that both the BNNT and the Au

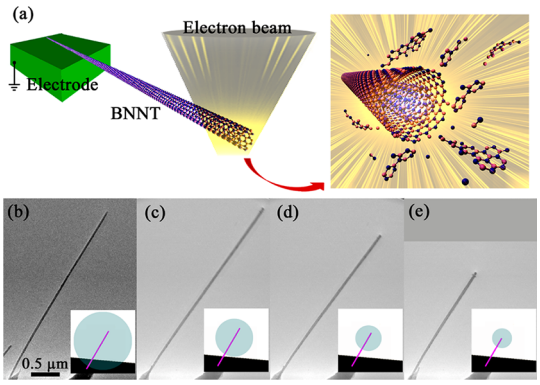

Figure 1. (a) Schematic drawing of the tube shells tearing and subsequent detaching of a cantilevered BNNT at its free end when it is irradiated under electron beam. (b−e) TEM images showing that a cantilevered BNNT was gradually shortened under EBI when beam density was gradually increased by decreasing a beam size. The insets schematically show the gradual decrease of electron beam (cyan circle) size and its relative positions against the Au electrode (black trapezoid) and the BNNT (magenta line).

electrode edge (supporting the BNNT) were irradiated. The BNNT was found to exhibit a clear contour under TEM observation (Figure 1b). When the beam size was decreased, with the Au electrode edge being left outside the beam area, and electron beam started to irradiate only the cantilevered nanotube section, its contour suddenly became slightly blurred (Figure 1c). While the beam density continued to increase to about 0.8 A/cm^2 by further decreasing the beam size, the tube started to gradually shorten with its material being locally "evaporated" from the free end (Figure 1d,e and video S1 in Supporting Information). The evaporation could be easily speeded up and slowed down or even stopped by adjusting the electron beam size and increasing or decreasing the beam density (see video S1 in Supporting Information). It means that only after the electron beam density becomes higher than a threshold value can the evaporation of BNNT take place and its rate increases with beam density. During the evaporation, some small particles seemed to appear at the nanotube end (Figure 1e).

In order to get more details on what happened to BNNTs during the regarded evaporation, the tubes were observed at higher TEM magnifications, while they were gradually shortened. Figure 2a,b depicts the TEM images of another cantilevered BNNT before and after it was shortened from 9.3 to 6.1 μm, as measured from the Au electrode edge to the nanotube free end. Figure 2c−f gives the details. It can be seen that the tube shells were torn into small pieces that repelled each other and then were detached from the nanotube under such repulsion (also see video S2 in Supporting Information). Interestingly, the tearing only took place locally at the tip end and the nanotube remained intact tens of nanometers away from the tip end, even

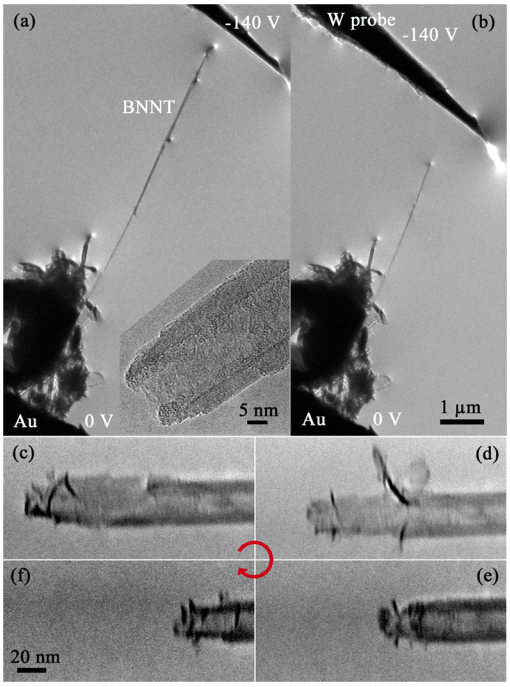

Figure 2. (a,b) TEM images showing a cantilevered BNNT protruding from the Au electrode edge when it was shortened from 9.3 μm (a) to 6.1 μm (b) under EBI. The inset in (a) is a high-resolution TEM image of the free end of the BNNT after it was shortened. Its diameter was measured to be ~30 nm. (c−f) TEM images revealing that the tube shells at the free end were torn into graphene-like pieces and then removed during tube shortening. In order to observe the positively charged BNNT at high magnifications as in (c−f), a W probe with −140 V voltage applied to it was used in (a,b) to stabilize the tube by Coulomb attraction.

though the intact nanotube section was under electron irradiation, as well. With tearing and detaching taking place continuously, the BNNT was gradually shortened from its tip end. However, the shortening could not proceed endlessly; rather it stopped at a certain nanotube length if the electron beam density was fixed. It means that, for a given electron beam density, only after the nanotube length is higher than a threshold value can the evaporation process take place.

When the shortening stopped at a certain nanotube length, a further increase of electron beam density was needed to initiate it again. Therefore, the threshold value of electron beam density for the evaporation process increased when the nanotube length decreased; in other words, the threshold value of nanotube length decreased when the electron beam density increased. For the BNNT in Figure 2, the threshold beam density was found to be about 2000 A/cm^2 when the tube was 6.1 μm long; this value decreased with the nanotube length increase. The lowest beam density for the evaporation process was observed to be only about 0.1 A/cm^2 in our experiments. It can be concluded that the shortening process depends on both beam density and cantilevered BNNT length. Only after they are larger than the threshold values can the shortening process take place, and the threshold value of one of these parameters decreases with an increase in the value of the other one. The above phenomena were repeatable for 11 BNNTs. High-resolution TEM image inset in Figure 2a indicates that the BNNT exhibits well-structured tubular shells and an open rough end after being shortened.

What is the physical mechanism responsible for the above tube shortening is the question we are concerned with now. Even though an external pulling electric field was applied *via* a negatively biased W probe for the BNNT in Figure 2, the nanotube evaporations in our experiments were mostly detected without an external pulling electric field. Thus field evaporation due to external pulling electric field can be excluded.[14,15] The tube shortening should be caused by electron beam irradiation. Knock-on atom displacement is thought to be one of the primary effects responsible for the structural damage of irradiated targets,[5−7] especially for the targets consisting of light atoms and irradiated with high-energy electron beam in a high vacuum, just like in the case of our experiments. However, it cannot explain the observed herein BNNT shortening under EBI. First, knock-on atom displacement results from the elastic collisions with incident electrons, so it only depends on the characteristics of the incident electron beam and targeting atoms.[9,16] This cannot explain why the tube shortening depends on the length of cantilevered BNNTs, as well as why the tube failure only takes place locally at the tube tip ends. Second, knock-on atom displacement in BN nanostructures primarily results in the sputtering of B or N atoms[8,9,17] but not in the tearing of nanotube shells and the subsequent detaching of small BN sheets/clusters, as observed in our experiments. Finally, the severe and quick failure of thick multiwalled BNNTs based on knock-on atom displacement requires a beam density as high as about 10^5 A/cm^2,[13] while in our experiments, the tube failure was observed at a beam density even as low as 0.1 A/cm^2. Therefore, some other mechanism should be primarily responsible for the observed phenomenon.

Figure 3 illustrates the electrostatic interactions between an irradiated BNNT and an electrically biased tungsten probe. It can be seen that the nanotube was electrostatically attracted by the probe if the probe was negatively biased and was repelled if the probe was positively biased. It means that the BNNTs irradiated under an electron beam were positively charged.[18] Considering the facts that the small BN sheet pieces repelled each other and were soon detached from the BNNT under repulsion during the tube shortening, the tearing of BNNT shells in Figure 2 is thought to be primarily caused by Coulomb repulsion due to the positive charging of BNNTs under EBI, and the evaporation process is suggested to be the local Coulomb explosion (LCE) of BNNTs at their free ends when they are profoundly charged.

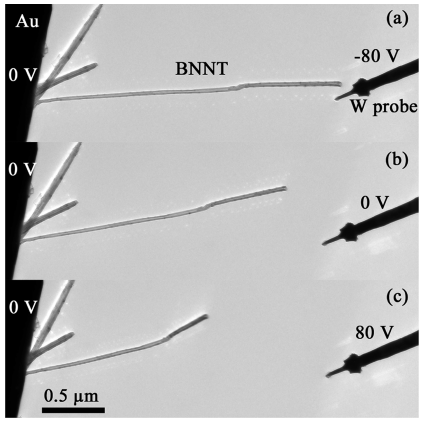

Figure 3. TEM images showing the Coulomb interaction between an electron-irradiated BNNT and a biased W probe with −80 V (a), 0 V (b), and 80 V (c) voltage applied.

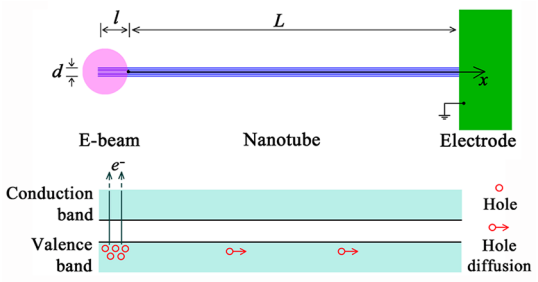

Figure 4. Schematic drawing of a cantilevered BNNT protruding from a grounded electrode and irradiated by an electron beam and its energy band diagram showing the positive charge production and hole diffusion.

Local Coulomb explosion due to profound positive charging can well explain the observed phenomena. Positive charging of BNNTs is thought to be sourced by secondary electron emission with a secondary yield larger than 1, and its rate is proportional to the density of primary electron beam.[19] Since BNNTs were connected to a grounded Au electrode in our experiments, the produced positive charges can be simultaneously drained away through charge (hole) diffusion along a nanotube to the electrode. The rate of charge draining depends on the nanotube length if the diffusion coefficient of charges is fixed. The shorter the nanotube is, the faster the charges will be drained off. The charge accumulation in the irradiated area depends on both the charge sourcing and draining, so the charging of an irradiated BNNT and its local Coulomb explosion depends not only on electron beam density but also on nanotube length. In order to accumulate enough charges for Coulomb explosion, electron beam density should be high enough to ensure a fast charge sourcing and the nanotube should be long enough to ensure a slow charge draining. These ideas are in good agreement with our experimental observations that only after electron beam density and nanotube length are larger than threshold values can the tube shortening takes place.

To accumulate positive charges in an irradiated BNNT, electron conduction along the nanotube from the Au electrode to irradiated tube section should be forbidden; otherwise, positive charges will be neutralized by electrons flowing from the electrode. Since the electrons in the valence band of a BNNT can be excited to its conduction band under electron irradiation (which will induce electron conduction along the BNNT), significant positive charge accumulation and Coulomb explosion cannot take place when the whole cantilevered tube section (from the connecting point with the Au electrode edge to the tube free end) is under electron irradiation. This agrees well with our observations in Figure 1b−e, where the BNNT became blurred and LCE took place only after the beam size was decreased so that only a part of the cantilevered tube section was irradiated by the electron beam. The blurring of nanotube contour is thought to be caused by BNNT vibration due to significant positive charging.

To describe the positive charge accumulation at the irradiated tube section, and to verify quantitative agreements between our observed phenomena and local Coulomb explosion due to profound positive charging, we propose a theoretical model based on the diffusion of electron-irradiation-induced holes along a BNNT. In this model, as schematically shown in Figure 4, a cantilevered BNNT with a diameter of d is connected to a grounded electrode at the tube's right end. The nanotube is partially irradiated under an electron beam from its left end with the length of tube section under irradiation being l, and the length of the section free of electron irradiation being L. As introduced above, the tube section under electron irradiation is positively charged. A portion of the positive charges are assumed to be in the form of mobile holes that can diffuse along the nanotube to the electrode, so that the positive charges can be partially drained off. To calculate the accumulated charges, we have to consider the transport of holes from the irradiated tube section, where they are produced, to the electrode through the tube section free of irradiation.

Considering that the electrons in the conduction band of the tube section free of electron irradiation are negligible for wide band gap BNNTs, electron−hole recombination and electron conduction are neglected here. Since a temperature increase of only ~28 K was measured for a highly thermoconductive material under the electron beam irradiation analogous to that used in our experiments,[20] the effect of heating due to electron beam irradiation is neglected, as well. The positive charging at the irradiated tube section increases its potential relative to the electrode, so an internal electric field is built along the nanotube. Therefore, the transport of holes along the tube is now governed by the electric-field-assisted

diffusion equation considering both the diffusion and drifting of holes:[21]

$$\frac{\partial n(x,t)}{\partial t} = D\frac{\partial^2 n(x,t)}{\partial x^2} - \mu E(t)\frac{\partial n(x,t)}{\partial x} \quad (1)$$

where $n(x,t)$ is the line density of holes at the position x and time t along the nanotube section free of irradiation. D is diffusion coefficient of holes in BNNTs, and $\mu = eD/k_BT$ is hole mobility with e being electron charge, k_B is Boltzmann constant, and T = 300 K is the room temperature. $E(t)$ is the strength of electric field at time t, which is assumed to be constant along the nanotube section free of irradiation and determined by the charges at the irradiated tube section [$Q(t)$]. In the case of $d \sim l \ll L$, the charges at the irradiated tube section can be considered to be uniformly distributed at the volume with a diameter l, so its potential can be written as $V(t) = 2k_eQ(t)/l$ with $k_e = 9 \times 10^9$ Nm^2/C^2 being the Coulomb constant, and the electric field strength is

$$E(t) = 2k_eQ(t)/lL \quad (2)$$

The accumulated charges at the irradiated tube section [$Q(t)$] are determined by both the charge sourcing due to secondary electron emission and the charge draining due to hole diffusion. The charge sourcing per unit time is $(\delta - 1)j_0S$ if the electron backscattering is negligible, where δ is secondary yield with a value larger than 1, j_0 is the density of electron beam and $S = dl$ is the cross-sectional area of the tube section under EBI. The charge draining per unit time is $j(t)e$ with $j(t)$ being the flux of hole diffusion at $x = 0$. Assuming that the electron irradiation starts at $t = 0$, the quantity of the accumulated charges at the irradiated tube section is calculated by

$$Q(t) = \int_0^t ((\delta - 1)j_0S - j(t')e)dt' \quad (3)$$

where the flux of hole diffusion at $x = 0$ can be written as

$$j(t) = -D\frac{\partial n(0,t)}{\partial x} + \mu E(t)n(0,t) \quad (4)$$

The ratio of the mobile holes to all accumulated charges at the irradiated tube section [$Q(t)$] is assumed to be α, then the line density of holes at the irradiated tube section ($x = 0$) is

$$n(0,t) = \alpha Q(t)/el \quad (5)$$

Since electron irradiation starts at $t = 0$, we have

$$n(x,0) = 0 \quad (6)$$

Taking eqs 5 and 6 as the boundary and initial conditions, eqs 1−4 were numerically solved by finite differential method, and the time evolution of accumulated charges at the irradiated tube section [$Q(t)$] was obtained.

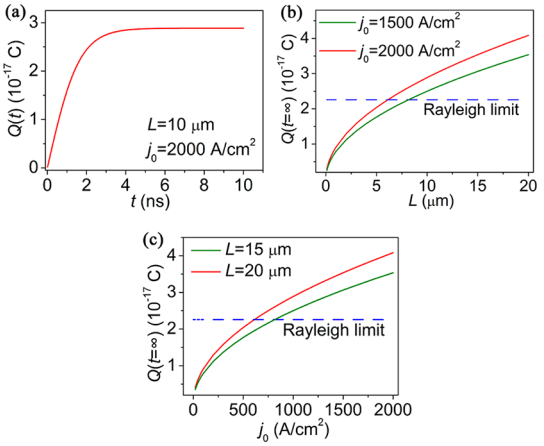

Figure 5. Calculated results based on the theoretical model. (a) Time evolution of accumulated charges [$Q(t)$] at the irradiated tube section when a nanotube length (L) is 10 μm and beam density (j_0) is 2000 A/cm^2. (b) Dependence of saturated charges [$Q(t = \infty)$] on the nanotube length for a given beam density. (c) Dependence of saturated charges on beam density for a given nanotube length.

Figure 5 gives the calculated results along the above-discussed model, where μ = 27 cm^2/V·s,[22] δ = 2, α = 0.004, and $d = l$ = 30 nm were used. The time evolution of the accumulated charges in a 10 μm cantilevered BNNT with electron beam density of 2000 A/cm^2 is shown in Figure 5a. It can be seen that the accumulated charge increases first with time and saturates at a value in the order of 10^{-17} C at a time scale of only a few nanoseconds, during which the charge draining keeps increasing until it balances the charge sourcing. So the charging of BNNTs under EBI is a very fast process that can be completed in several nanoseconds. The maximum quantity of charges that the irradiated tube section may hold is given by the Rayleigh limit $Q_{Rayleigh} = 8\pi(\gamma\varepsilon_0 r^3)^{1/2}$,[23,24] where γ = 27 mN/m is the surface tension coefficient of BNNTs,[25] ε_0 is the permittivity of free space, and $r = l/2$ = 15 nm is the radius of irradiated tube volume. The Rayleigh limit was calculated to be 2.3 $\times$ 10^{-17} C. When the accumulated charge is larger than the Rayleigh limit, Coulomb explosion will take place.

Figure 5b shows the dependence of the saturated charge [$Q(t = \infty)$] on the nanotube length when electron beam density is fixed. It can be seen that $Q(t = \infty)$ increases with BNNT length for a given beam density. For a beam density of 1500 A/cm^2, $Q(t = \infty)$ becomes larger than the Rayleigh limit when the nanotube length is larger than a threshold value of 8.1 μm, so Coulomb explosion would take place there; otherwise, $Q(t = \infty)$ is smaller than the Rayleigh limit and Coulomb explosion would not occur. When a beam density increases to 2000 A/cm^2, the threshold value of tube length decreases to 6.0 μm. This is in good agreement with our observation in Figure 2b, where LCE stopped at a tube length of 6.1 μm when electron beam density was 2000 A/cm^2.

The requirements of free-standing BNNTs and a cantilevered tube length as long as several micrometers for LCE can explain why LCE was not observed before. The dependence of $Q(t=\infty)$ on electron beam density for a given tube length is shown in Figure 5c, where $Q(t=\infty)$ increases with electron beam density, as well. It indicates that only after electron beam density is higher than 820 A/cm^2 can $Q(t=\infty)$ be larger than the Rayleigh limit and Coulomb explosion takes place when a nanotube length is 15 μm. The threshold value decreases to 610 A/cm^2 when a nanotube is 20 μm long. Those results agree well with our observations that the threshold value of beam density or BNNT length decreases with increasing the corresponding value of the competitive parameter. Therefore, the model successively and in a quantitative manner describes the observed LCE. It should be mentioned that some cantilevered BNNTs in our experiments did not directly connect to a Au electrode as considered in the model but protruded from a large nanotube assembly that adhered to the edge of a Au electrode. In this case, the transport distance of holes for charge draining can be much longer than the cantilevered nanotube length, so the required beam density for LCE can be much lower than that predicted by the model based on the cantilevered nanotube length and can reach a low value of about 0.1 A/cm^2.

The local occurrence of Coulomb explosion at the tip end of BNNTs can be well-understood based on the following two considerations. First, the tip end has the longest distance from the electrode, so it has the lowest rate of charge draining and the highest saturated charge. This is verified in Figure 5b, where the saturated charge increases with a distance between the irradiated tube section and the electrode. Second, BNNTs have rough open ends, as shown in Figure 2a, so a tip end is expected to have the smaller Rayleigh limit as compared to the other tube sections due to the structural imperfections. The two factors can both make the Rayleigh limit to be first satisfied at the tip end and Coulomb explosion to locally occur there. It is noted that even though the LCE induced by profound positive charging is thought to be primarily responsible for the observed phenomena, possible minor contributions of the knock-on effect cannot be fully ruled out.

Since the materials of irradiated targets can be locally removed during LCE, this phenomenon may open up a new promising way for nanostructure engineering. Taking our particular experimental setup as an example, the length of cantilevered BNNTs can be well-controlled by LCE, so it provides a new method for engineering BNNT length. As compared to the knock-on effect-based engineering of BNNTs, where a beam density as high as 10^5 A/cm^2 or an irradiation time as long as 0.5−2 h (for a lower beam density of 300 A/cm^2) has been required,[13] the engineering based on LCE takes just a few seconds and can be performed at a beam density of as low as 0.1 A/cm^2 for comparatively long and thick tubes. The engineering can be easily speeded up and slowed down or even stopped by just adjusting an electron beam size to increase or decrease the beam density. More importantly, in contrast with the knock-on effect-based engineering that can only be controlled by tuning the characteristics of incident electron beam and targeting atoms, LCE-based engineering can be controlled in a more versatile way by controlling the characteristics of surrounding electrical environments of an irradiated target, which determine the charge draining from it, in addition to the incident electron beam and targeting atom factors. For example, along with the nanotube length factor, as shown above, the charging of BNNTs in our experiments is expected to depend on the voltage of the electrode, as well (Figure 4). This can change the strength of electric field in BNNTs and thus speed up or slow down the transportation of holes along them, so their LCE can also be controlled by tuning the electrode voltage. As indicated by the theoretical model, profound positive charging and subsequent LCE can also take place for other dielectric nanostructures, as long as they have proper secondary electron yield, charge diffusion constant, and surface tension coefficient. Therefore, the LCE-based engineering is expected to work for other dielectric nanostructures, as well.

CONCLUSION

In conclusion, we have demonstrated that Coulomb explosion can take place in a controllable manner at the nanoscale and can be used to engineer a nanostructure. Cantilevered BNNTs irradiated with an electron beam with high enough intensity were observed to be gradually shortened with the tubular shells at the tube ends being torn into pieces and then removed. This was attributed to local Coulomb explosion that resulted from profound positive charging under EBI. The LCE was found to depend on the length of cantilevered nanotubes, as well as on electron beam density. Only after electron beam density and the cantilevered tube length were larger than threshold values can LCE take place, and the threshold value for one of the parameters decreases with increasing the value of the other one. A theoretical model based on the diffusion of electron-irradiation-induced holes along a BNNT was proposed to describe its positive charge accumulation. This could well explain the observed LCE. LCE in our particular experimental setup provides an efficient and versatile method to engineer the length of BNNTs as well as other dielectric nanostructures. As compared to the knock-on effect-based engineering where a long irradiation time or a high beam density is required, the presently designed

technique needs just a few seconds and a beam density as low as 0.1 A/cm^2. It is envisaged to open up a new and promising way for the nanostructure engineering.

METHODS

The experiments were *in situ* performed at room temperature inside a JEOL 3100FEF high-resolution TEM equipped with a scanning tunneling microscope (STM)-TEM "Nanofactory Instruments" holder. "Snow-white" entirely pure BNNTs synthesized by an induction heating method were used in our experiments.[26] The BNNTs were introduced into TEM by first dipping a Au wire (electrode) about 0.3 mm thick into a BNNT powder and then mounting this wire onto the STM-TEM holder. Under TEM observations, many individual cantilevered BNNTs directly protruding from the Au wire edge or protruding from a nanotube assembly at the Au wire edge can be easily found. In order to observe what happens to BNNTs under electron beam irradiation, the cantilevered BNNTs were irradiated with a 300 kV electron beam while the Au wire electrode was grounded. The changes of nanotube structure under electron irradiation were directly recorded under TEM imaging.

Conflict of Interest: The authors declare no competing financial interest.

Acknowledgment. This work was supported by the 973 program of MOST (2013CB933604), FANEDD (201241), and NSF (60925003) of China, and the International Center for Materials Nanoarchitectonics (MANA) of the National Institute for Materials Science (NIMS), Japan.

Supporting Information Available: Two videos (videos S1 and S2) showing the local Coulomb explosion of BNNTs under electron beam irradiation. Video S1 was taken when electron beam density was changed by adjusting beam size. This material is available free of charge *via* the Internet at http://pubs.acs.org.

REFERENCES AND NOTES

1. Golberg, D.; Bando, Y.; Tang, C. C.; Zhi, C. Y. Boron Nitride Nanotubes. *Adv. Mater.* **2007**, *19*, 2413–2432.
2. Wei, X. L.; Wang, M. S.; Bando, Y.; Golberg, D. Tensile Tests on Individual Multi-Walled Boron Nitride Nanotubes. *Adv. Mater.* **2010**, *22*, 4895–4899.
3. Banhart, F.; Li, J. X.; Terrones, M. Cutting Single-Walled Carbon Nanotubes with an Electron Beam: Evidence for Atom Migration Inside Nanotubes. *Small* **2005**, *1*, 953–956.
4. Wei, X. L.; Chen, Q.; Liu, Y.; Peng, L. M. Cutting and Sharpening Carbon Nanotubes using a Carbon Nanotube `Nanoknife'. *Nanotechnology* **2007**, *18*, 185503.
5. Krasheninnikov, A. V.; Banhart, F. Engineering of Nanostructured Carbon Materials with Electron or Ion Beams. *Nat. Mater.* **2007**, *6*, 723–733.
6. Krasheninnikov, A. V.; Nordlund, K. Ion and Electron Irradiation-Induced Effects in Nanostructured Materials. *J. Appl. Phys.* **2010**, *107*, 071301.
7. Banhart, F. Irradiation Effects in Carbon Nanostructures. *Rep. Prog. Phys.* **1999**, *62*, 1181–1221.
8. Zobelli, A.; Ewels, C. P.; Gloter, A.; Seifert, G.; Stephan, O.; Csillag, S.; Colliex, C. Defective Structure of BN Nanotubes: From Single Vacancies to Dislocation Lines. *Nano Lett.* **2006**, *6*, 1955–1960.
9. Zobelli, A.; Gloter, A.; Ewels, C. P.; Colliex, C. Shaping Single Walled Nanotubes with an Electron Beam. *Phys. Rev. B* **2008**, *77*, 045410.
10. Stéphan, O.; Bando, Y.; Loiseau, A.; Willaime, F.; Shramchenko, N.; Tamiya, T.; Sato, T. Formation of Small Single-Layer and Nested BN Cages under Electron Irradiation of Nanotubes and Bulk Material. *Appl. Phys. A: Mater. Sci. Process.* **1998**, *67*, 107–111.
11. Wei, X. L.; Wang, M. S.; Bando, Y.; Golberg, D. Post-Synthesis Carbon Doping of Individual Multiwalled Boron Nitride Nanotubes *via* Electron-Beam Irradiation. *J. Am. Chem. Soc.* **2010**, *132*, 13592–13593.
12. Wei, X. L.; Wang, M. S.; Bando, Y.; Golberg, D. Electron-Beam-Induced Substitutional Carbon Doping of Boron Nitride Nanosheets, Nanoribbons, and Nanotubes. *ACS Nano* **2011**, *5*, 2916–2922.
13. Celik-Aktas, A.; Stubbins, J. F.; Zuo, J. M. Electron Beam Machining of Nanometer-Sized Tips from Multiwalled Boron Nitride Nanotubes. *J. Appl. Phys.* **2007**, *102*, 024310.
14. Müller, E. W.; Tsong, T. T. *Field Ion Microscopy: Principles and Applications*; Elsevier: New York, 1969.
15. Wang, M. S.; Chen, Q.; Peng, L. M. Grinding a Nanotube. *Adv. Mater.* **2008**, *20*, 724–728.
16. Zobelli, A.; Gloter, A.; Ewels, C. P.; Seifert, G.; Colliex, C. Electron Knock-on Cross Section of Carbon and Boron Nitride Nanotubes. *Phys. Rev. B* **2007**, *75*, 245402.
17. Jin, C. H.; Lin, F.; Suenaga, K.; Iijima, S. Fabrication of a Freestanding Boron Nitride Single Layer and Its Defect Assignments. *Phys. Rev. Lett.* **2009**, *102*, 195505.
18. Golberg, D.; Mitome, M.; Kurashima, K.; Zhi, C. Y.; Tang, C. C.; Bando, Y.; Lourie, O. *In Situ* Electrical Probing and Bias-Mediated Manipulation of Dielectric Nanotubes in a High-Resolution Transmission Electron Microscope. *Appl. Phys. Lett.* **2006**, *88*, 123101.
19. Gross, B.; von Seggern, H.; West, J. E. Positive Charging of Fluorinated Ethylene Propylene Copolymer (Teflon) by Irradiation with Low-Energy Electrons. *J. Appl. Phys.* **1984**, *56*, 2333–2336.
20. Kawamoto, N.; Wang, M.-S.; Wei, X. L.; Tang, D. M.; Murakami, Y.; Shindo, D.; Mitome, M.; Golberg, D. Local Temperature Measurements on Nanoscale Materials Using a Movable Nanothermocouple Assembled in a Transmission Electron Microscope. *Nanotechnology* **2011**, *22*, 485707.
21. Miotello, A.; Dapor, M. Slow Electrons Impinging on Dielectric Solids. II. Implantation Profiles, Electron Mobility and Recombination Processes. *Phys. Rev. B* **1997**, *56*, 2241–2247.
22. He, B.; Zhang, W. J.; Yao, Z. Q.; Chong, Y. M.; Yang, Y.; Ye, Q.; Pan, X. J.; Zapien, J. A.; Bello, I.; Lee, S. T.; *et al.* p-Type Conduction in Beryllium-Implanted Hexagonal Boron Nitride Films. *Appl. Phys. Lett.* **2009**, *95*, 252106.
23. Rayleigh, L. On the Equilibrium of Liquid Conducting Masses Charged with Electricity. *Philos. Mag.* **1882**, *14*, 184–186.
24. Taflin, D. C.; Ward, T. L.; Davis, E. J. Electrified Droplet Fission and the Rayleigh Limit. *Langmuir* **1989**, *5*, 376–384.
25. Yum, K.; Yu, M. F. Measurement of Wetting Properties of Individual Boron Nitride Nanotubes with the Wilhelmy Method Using a Nanotube-Based Force Sensor. *Nano Lett.* **2006**, *6*, 329–333.
26. Zhi, C. Y.; Bando, Y.; Tan, C. C.; Golberg, D. Effective Precursor for High Yield Synthesis of Pure BN Nanotubes. *Solid State Commun.* **2005**, *135*, 67–70.